Journal of Photochemistry and Photobiology A: Chemistry 322 (2016) 53–59

Contents lists available at ScienceDirect

Journal of Photochemistry and Photobiology A: Chemistry

journal homepage: www.elsevier.com/locate/jphotochem

Isomerization and dissociation of 2,3-dihydrofuran (2,3-DHF) induced by infrared free electron laser

M. Matsubara[a,1], F. Osada[a,2], M. Nakajima[b,3], T. Imai[b], K. Nishimura[a], T. Oyama[a], K. Tsukiyama[a,*]

[a] Department of Chemistry, Faculty of Science, Tokyo University of Science, 1-3 Kagurazaka, Shinjuku, Tokyo 162-8601, Japan
[b] IR Free Electron Laser Research Center, Research Institute for Science and Technology (RIST), Tokyo University of Science, 2641 Yamazaki, Noda, Chiba 278-8510, Japan

ARTICLE INFO

Article history:
Received 13 January 2016
Received in revised form 16 February 2016
Accepted 17 February 2016
Available online 23 February 2016

Keywords:
Free electron laser
Isomerization
Multiphoton absorption
Quantum chemical calculation

ABSTRACT

We investigated infrared multiphoton dissociation and isomerization reactions of 2,3-dihydrofuran (2,3-DHF), cyclopropanecaboxaldehyde (CPCA) and crotonaldehyde (CA) with free electron laser at Tokyo University of Science (FEL-TUS). From 2,3-DHF as a starting material, CPCA and CA were the main isomerization products. From the measured [CPCA]/[CA] ratio, the equivalent temperature for the vibrationally hot 2,3-DHF was estimated to be 1300–1500 K. From CPCA, both 2,3-DHF and CA were detected as isomerization products. No isomerization reaction from *trans*-CA to CPCA and 2,3-DHF was recognized and the dissociation to propylene was the dominant process. The experimentally identified reaction pathways are well explainable by quantum chemical calculations at the MP2/cc-pVDZ level.

1. Introduction

Thermal reactions of cyclic ether at high temperatures have been the subjects of extensive experimental and theoretical investigations. In particular, dihydrofuran (DHF) compounds have attracted much attention because of their simple molecular structure. Lifshitz and coworkers [1–8] reported a series of experiments on the shock-initiated reactions of oxygen-containing five-membered rings. The pyrolysis of 2,5-DHF over the temperature range 880–1480 K induces the dehydrogenation reaction to generate hydrogen and furan [4]. On the other hand, two reaction channels, isomerization and dissociation, exist for the pyrolysis of 2,3-DHF [5]: The dissociation reaction yields ethylene and ketene, whereas unimolecular isomerization produces c-C_3H_5CHO (cyclopropanecaboxaldehyde, hereafter denoted as CPCA) as a main product. An isomerization process to $CH_3CH{=}CHCHO$ (crotonaldehyde, hereafter denoted as CA) was later identified in the experiment employing a furan derivative as a starting material [6]. Recently, Karunatilaka et al. reported the production of CPCA and CA in a discharge plasma of 2,3-DHF [9].

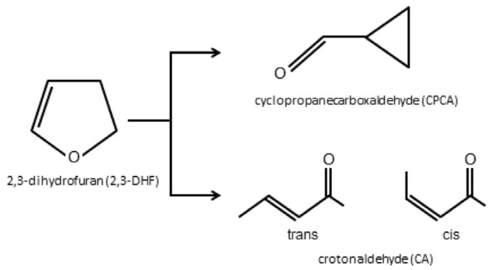

Infrared multiphoton excitation (IRMPE) is a general technique available for driving unimolecular isomerization as well as dissociation reactions. For example, Chowdhury and Mittal [10] reported IR multiphoton dissociation dynamics of 2,5-DHF by a pulsed CO_2 laser, in which hydrogen and furan, the same products as the shock tube experiment, were identified as primary products. The use of infrared free electron laser (IR-FEL) for the study of infrared multiphoton dissociation (IRMPD) seems to be much more attractive than CO_2 laser due to, first, the wide wavelength tunability covering the whole finger print region [11–14]. This feature allows us to inspect the wavelength dependence of various photochemical processes, in other words, to excite different vibrational modes selectively in the molecules. In fact, mass spectrometry with IR-FEL as a tunable light source has been one of

---

[*] Corresponding author. Fax: +81 3 5261 4631.
E-mail address: tsuki@rs.kagu.tus.ac.jp (K. Tsukiyama).

[1] Present address: Hikari Tsushinn Co., Ltd, 1-4-10 Nishi-Ikebukuro, Toshima, Tokyo 171-0021, Japan.

[2] Present address: Riken Keiki Co., Ltd, 2-7-6 Komamezawa, Itabashi, Tokyo 172-8744, Japan.

[3] Present address: The University of Tokyo, 3-8-1 Komaba, Meguro, Tokyo 153-8902, Japan.

http://dx.doi.org/10.1016/j.jphotochem.2016.02.014
1010-6030/

the most powerful spectroscopic technique for studying the molecular structure and reaction mechanism of molecules, ions and clusters in the gas phase [15,16]. On the other hand, employing a grating-tuned CO_2 laser combined with an FTICR (Fourier transform ion cyclotron resonance) mass spectrometer, Ehsan et al. succeeded in obtaining an IRMPD spectrum which is narrower than that taken with IR-FEL [17].

FEL-TUS (infrared free electron laser at Tokyo University of Science) possesses a unique temporal pulse structure containing the train of pico-second pulses. In our previous experiments [11,12], we showed that this could enhance the efficiency of ladder climbing of the infrared photons because the interval between successive pulses is short enough compared with the collisional interval of molecules in the gas phase, which may minimize the collisional relaxation of the internal energy and increase the possibility of IRMPE. In the current paper, we present the results of IRMPE of 2,3-DHF by FEL-TUS. The experimental results will be discussed in connection with the calculation.

2. Experimental

The structure and the characteristics of FEL-TUS have been described previously [11]. In brief, the wavelength is variable within the mid-infrared region of 5–16 μm (625–2000 cm^{-1}). FEL-TUS provides two kinds of laser pulses, i.e. so-called macropulse and micropulse. The macropulse has a duration of $\sim$2 μs and a repetition rate of 5 Hz throughout the operation. This macropulse consists of a train of micropulses with a duration of $\sim$2 ps. The interval of two consecutive micropulses is 350 ps which corresponds to the RF frequency (2856 MHz) employed for the linear accelerator. Accordingly, one macropulse contains $\sim$6000 micropulses. The irradiation condition is similar to that of our previous experiment [11,12]. The infrared light beam from FEL-TUS was reflected on the concaved mirror with a focal length of 500 cm, and the reflected beam was focused into the center of a reaction cell (diameter; 25 mm, length; 120 mm, windows; BaF_2) by a BaF_2 lens with a focal length of typically 30 cm. The energy of the laser pulse was monitored with an energy meter (Gentec, ED-500) and the typical pulse energy was 8–10 mJ/macropulse. However, depending on the daily condition of FEL, the lower pulse energy ($\sim$5 mJ/macropulse) was provided in a given machine time. The average fluence is estimated to be $\sim$1 J/cm^2. The energy resolution of FEL-TUS is 1.0–1.5% of the output wavenumbers.

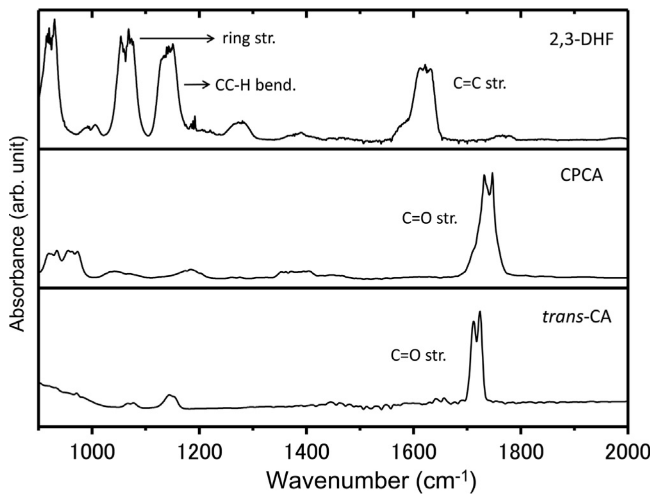

Fig. 1. IR absorption spectra of 2,3-DHF (upper trace; 2.3 Torr), CPCA (middle trace; 2.6 Torr), and *trans*-CA (lower trace; 2.3 Torr).

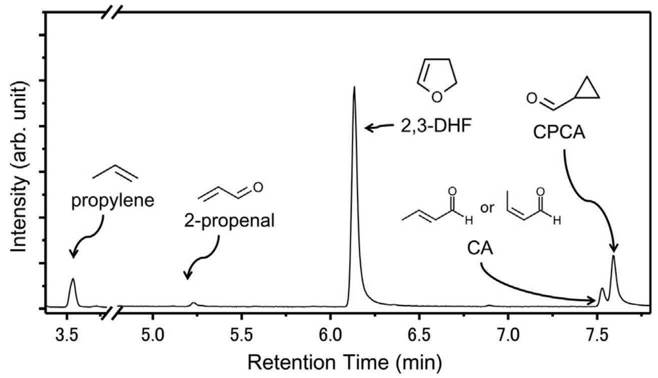

Fig. 2. Typical gas chromatogram of the sample gas after irradiation of FEL at $\sim$1580 cm^{-1} at room temperature. Parent molecule: 2,3-DHF. Initial pressure: 0.2 Torr. Irradiation time: 1 h (18000 shots). A similar spectrum is obtained after irradiation of FEL at $\sim$1040 cm^{-1}.

2,3-DHF (Wako Pure Chemical, >98% purity), CPCA (Tokyo Chemical Industry Co., >97% purity), *trans*-CA (Wako Pure Chemical, >99% purity) were used after degasification without any purification. Infrared absorption spectra of samples were measured using a FT-IR infrared spectrometer (JASCO, model 615). Quantitative analysis of the sample gas after irradiation of FEL was performed with a GC mass spectrometer (Shimadzu, GCMS-QP2010). The integrated intensity of the photo isomerization products, CPCA and CA, on the gas chromatogram is found to be proportional to the pressure of these compounds, respectively. Thus by drawing a working curve for each molecule and comparing the integrated areas on the gas chromatogram, the ratio of the products is evaluated with an estimated error of 10%.

3. Results and discussion

3.1. Irradiation of FEL to 2,3-DHF

Fig. 1 shows IR absorption spectra of 2,3-DHF (upper trace), CPCA (middle trace), and *trans*-CA (lower trace). For 2,3-DHF, a strong band near 1600 cm^{-1} is assigned to the C=C stretching mode. In the lower wavenumber region, two prominent bands near 1070 and 1140 cm^{-1} are assigned to the ring stretching and CC—H bending motions, respectively. On the other hand, only one prominent band around 1730 cm^{-1} exists for CPCA and CA corresponding to the C=O stretching mode.

Fig. 2 illustrates a typical gas chromatogram of the sample gas after the irradiation of FEL ($\sim$1580 cm^{-1}) to 2,3-DHF. A similar gas chromatogram is obtained at $\sim$1040 cm^{-1}. These wavenumbers correspond to the maximum efficiency for the isomerization reactions as discussed later. The peak near retention time of 6.2 min corresponds to the parent molecule, while two signals at 7.5 and 7.6 min to the photo isomerization products, namely, CA and CPCA, respectively. CA has *cis* and *trans* forms; only the latter is commercially available. The retention time and the mass pattern for the peak at 7.5 min are identical with that of *trans*-CA. Because the retention time of *cis*-CA is expected to be overlapped with *trans* conformer, we cannot estimate the ratio of *cis* to *trans* compound from the gas chromatogram only. In addition to the photo isomerization products, two photo dissociation products, propylene (retention time at 3.5 min) and 2-propenal (at 5.2 min) are identified.

Fig. 3a shows the action spectrum for the isomerization products, namely, the dependence of the isomerization reaction on the FEL wavenumber near the C=C stretching region of 2,3-DHF.

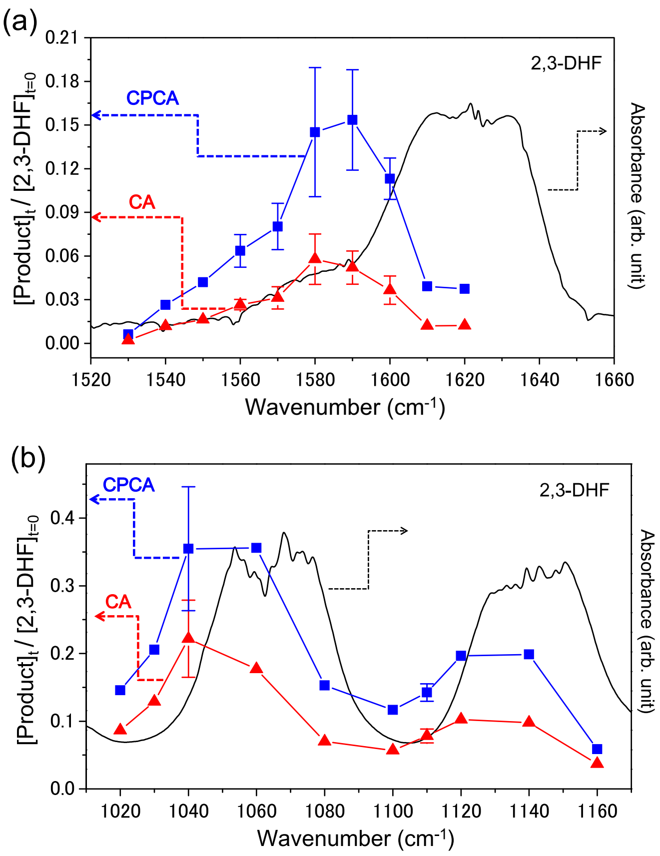

Fig. 3. Action spectrum for the isomerization products (blue: CPCA, red: CA) and FT-IR spectrum (black line) of the parent molecule in the vicinity of a) the C=C stretching and b) ring stretching and CC—H bending regions of 2,3-DHF. Parent molecule: 2,3-DHF. Initial pressure: 0.2 Torr. Irradiation time: 1 h (18000 shots). Horizontal axis corresponds to FEL wavenumber, while vertical axis to the ratio of partial pressure of the product to the initial pressure of 2,3-DHF. Error bar indicates a standard deviation for 2–4 measurements.

The vertical axis is defined as $[\text{product}]_t/[\text{2,3-DHF}]_{t=0}$, corresponding to the partial pressure of the isomerization products (CPCA and CA) divided by the initial pressure of 2,3-DHF. The black solid curve represents the FTIR spectrum of 2,3-DHF. The important findings are:

1. Each product exhibits, on the whole, a similar wavenumber dependence. The peak wavenumber is located ~40 cm^{-1} lower than the absorption peak of the C=C stretching motion, which is beyond the spectral resolution of FEL-TUS (FWHM ~20 cm^{-1} at 1590 cm^{-1}). Such spectral red-shift in the action spectrum, partly due to the anharmonicity of the vibrational energy levels, is a clear signature that the reaction is driven by IR multiphoton absorption [11,12].
2. CPCA is produced more preferentially than CA.

Fig. 3b shows the action spectrum in the vicinity of ring stretching and CC-H bending regions. The peaks of the reaction efficiency shifts to ~20 cm^{-1} lower than the IR absorption. It should be noted that, though CPCA is produced more efficiently than CA, the ratio of [CPCA]/[CA] is apparently smaller than that in Fig. 3a.

Fig. 4a plots the decay of 2,3-DHF (green circle) and the production of CPCA (blue square) and CA (red triangle) as a function of irradiation time at 1590 cm^{-1}; 1 h corresponds to 18000 macropulse shots. The partial pressure of 2,3-DHF is found to obey a first-order decay against irradiation time, while the generation of CPCA and CA is well described as a parallel first-order reaction with the same rate constant for the consumption of 2,3-DHF. From the fitting curves inserted in Fig. 4a, we evaluated [CPCA]/[CA] to be ~3.2 at 1590 cm^{-1}. A similar analysis for FEL wavenumber at 1040 cm^{-1} as shown in Fig. 4b results in [CPCA]/[CA] to be ~1.7 at 1040 cm^{-1}.

An extremely efficient isomerization scheme called “thermal explosion” has been identified in the experiments where the multiphoton process was conducted by TEA (transversely excited atmospheric) CO_2 laser [18]. Thermal explosion takes place when the heat released by isomerization exceeds the heat loss due to diffusion. One of the marked features of this process is that there exists a critical laser power above which one laser shot would suddenly trigger the isomerization. Under our experimental conditions, such explosion must be ruled out because the total pressure used in the present experiment (<1 Torr) was two orders of magnitude lower than the threshold pressure observed in the thermal explosion and because, furthermore, the focusing condition of FEL-TUS is much milder than that of TEA CO_2 laser where the fluecne of ~1 J/cm^2 was focused with a lens with f = 10–20 cm.

3.2. Irradiation of FEL to CPCA and *trans*-CA

From a typical gas chromatogram of the sample gas after the irradiation of FEL (~1720 cm^{-1}) to CPCA, propylene and a small amount of 2-propenal are identified as dissociation products. The yield of propylene formation after 1 h irradiation, $[\text{propylene}]_{t=1\,\text{h}}/[\text{CPCA}]_{t=0}$, is ~0.12. On the other hand, 2,3-DHF and CA are detected

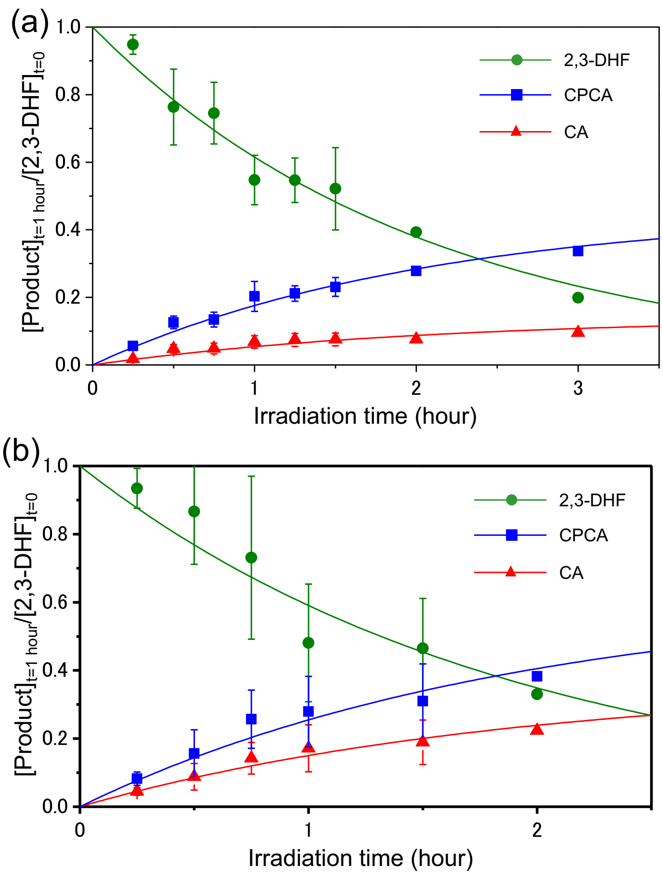

Fig. 4. Partial pressure of 2,3-DHF and the efficiency of dissociation and isomerization as a function of irradiation time at (a) 1590 cm^{-1} and (b) 1040 cm^{-1}. Parent molecule: 2,3-DHF. Initial pressure: 0.2 Torr. Error bar indicates a standard deviation for 2–4 measurements.

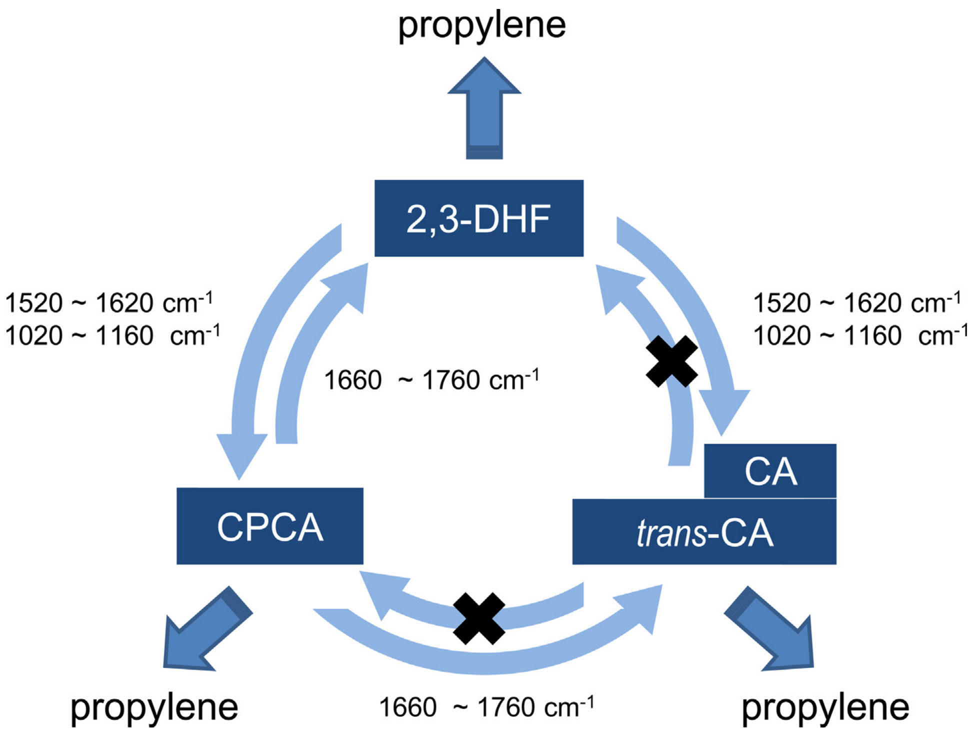

Fig. 5. The overall reaction paths induced by infrared multiphoton excitation among 2,3-DHF, CPCA and CA. The wavenumber represents the range of FEL-TUS output driving the conversion along the direction of the arrow.

as isomerization products. The yields of isomerization, $[\mathrm{CA}]_{t=1\,\mathrm{h}}/[\mathrm{CPCA}]_{t=0}$ and $[\text{2,3-DHF}]_{t=1\,\mathrm{h}}/[\mathrm{CPCA}]_{t=0}$ are ~0.07 and ~0.03, respectively. The efficiency of photo dissociation generating propylene is comparable to that of photo isomerization. The action spectra for CA and 2,3-DHF formation from CPCA exhibit a broad band from 1660 to 1760 cm^{-1} peaked at 1720–1730 cm^{-1}, which is ~10 cm^{-1} shifted to lower wavenumber compared with the C=O stretching mode of CPCA (see Fig. 1, middle trace).

The IRMPD of *trans*-CA produces primarily propylene (the yield: ~0.30 at 1700 cm^{-1} after 1 h irradiation) with a small amount of 2-propenal. No potential isomerization products such as 2,3-DHF and CPCA are detected. The action spectrum for propylene formation from *trans*-CA ranges from 1640 to 1740 cm^{-1} with a broad peak around 1700 cm^{-1}, which is located at ~20 cm^{-1} lower wavenumber side compared with the C=O stretching mode of *trans*-CA (see Fig. 1, bottom trace).

The important experimental findings are

I Propylene is detected as one of the major dissociation products from 2,3-DHF, CPCA and *trans*-CA.
II IRMPE of 2,3-DHF leads to isomerization into both CPCA and CA.
III IRMPE of CPCA leads to both 2,3-DHF and CA.
IV No isomerization reaction is detected in IRMPE of *trans*-CA.

The overall reaction paths among 2,3-DHF, CPCA, and CA is depicted in Fig. 5 together with the range of FEL wavenumber needed for the conversion. In the next section, these experimental results will be compared with quantum chemical calculations.

5. Quantum chemical calculation

The singlet potential energy surface for the unimolecular dissociation of 2,3-DHF to propylene and CO was surveyed by quantum chemical calculation at the second-order Møller–Plesset level of theory with the cc-pVDZ basis set (MP2/cc-pVDZ). Harmonic frequency calculations were carried out for all the reactants, products, and transition states (TSs), in order to make the zero-point energy correction for the electronic energies and to verify a TS to be located at a saddle point of the potential surface. The reaction path associated with a TS was examined by intrinsic reaction coordinate calculations for all the TSs. All the calculations were performed with the Molpro 2012.1 quantum chemistry package [19]. The minimum energy paths for the unimolecular dissociation of 2,3-DHF via different initial TSs are summarized in Fig. 6. Molecular structures of all the reactants and products and the TSs given in Fig. 6 are illustrated in Supplementary Figs. S1 and S2.

5.1. Dissociation and isomerization mechanism of 2,3-DHF

In the present survey, three TSs (TS1-3) connecting to the reactant 2,3-DHF were found, and each of them leads to a different product, CPCA or *cis*-CA or 3-butenal (3BA). Although two of the three TSs, leading to CPCA and *cis*-CA, have been already reported [8], that connecting between 2,3-DHF and 3BA was newly found in the present study. In the experiment, CA was detected as one of the main products though we could not identify whether CA is produced as a *trans*-conformer or a *cis*-conformer from the gas chromatogram only. Fig. 6, showing no TSs connecting 2,3-DHF with *trans*-CA, suggests that only *cis*-CA is directly produced from 2,3-DHF; the generation of *trans*-CA from 2,3-DHF is possible through TS9 via the hot 3BA. It is interesting to note that only the *trans* form was identified in the pulsed discharge of 2,3-DHF, which suggests that the discharge can provide product species with excess internal energy after the isomerization to convert between molecular conformations [9].

The IRMPE of 2,3-DHF can produce energized CPCA and *cis*-CA via TS1 and TS2, respectively, which would be stabilized by collisions with other molecules. Both of CPCA and *cis*-CA are connected to another product 3BA through TS5 and TS6, respectively. 3BA can dissociate to propylene + CO through a relatively low potential barrier (TS7; 33.17 kcal/mol). Once 3BA is produced by IRMPE of 2,3-DHF, it might immediately dissociate to

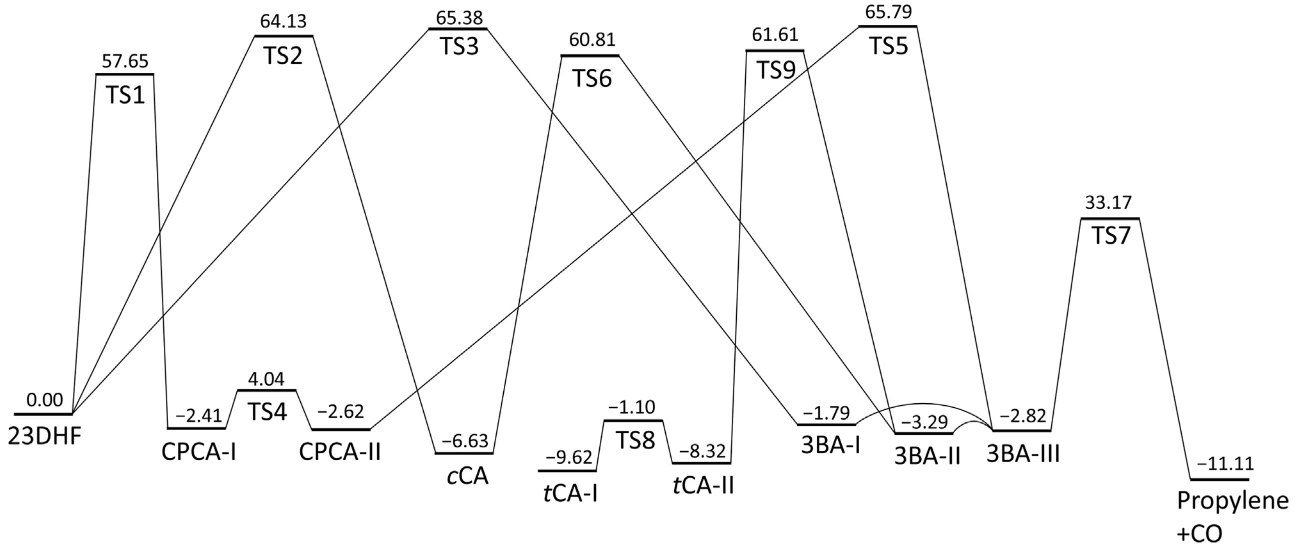

Fig. 6. Reaction paths from 2,3-DHF to propylene + CO obtained at the MP2/cc-pVDZ level of theory. 23DHF: 2,3-dihydrofuran, CPCA: cyclopropanecarboxaldehyde, CA: crotonaldehyde (*cis* and *trans*), 3BA: 3-butenal. Electronic energies with the zero-point vibration correction are given in kcal/mol, relative to that of 23DHF. Molecular structures are illustrated in Supplementary Figs. S1 and S2.

propylene + CO since the produced 3BA is enough energized to overcome the potential barrier. 3BA is also directly produced by the IRMPE of 2,3-DHF via TS3. It should be noted that all the conformers of 3BA can be interchanged to each other with a very small energy barrier.

5.2. Dissociation and isomerization mechanism of trans-CA and CPCA

No direct path from *trans*-CA to 2,3-DHF or CPCA was found, and *trans*-CA is only connecting to 3BA through TS9. This computational result is in good correspondence with the experimental fact that no isomerization reaction is detected in IRMPE of *trans*-CA. The photo-induced reaction of *trans*-CA would uniquely lead to propylene + CO via the intermediate of 3BA. Although the *cis*–*trans* interconversion of CA could not be treated with the present level of theory, it is ignorable for understanding the experimental results.

In the experiment, both 2,3-DHF and CA are detected from CPCA, while no TS connects CA with CPCA directly in the present computation. The production of CA from CPCA might proceed via a stepwise mechanism, i.e. via hot 2,3-DHF intermediate which further converts to *cis*-CA through TS2. On the other hand, the previous DFT calculation [8] exhibits the potential energy surface from CPCA to *cis*-CA isomerization. The possibility of direct *cis*-CA production cannot be excluded.

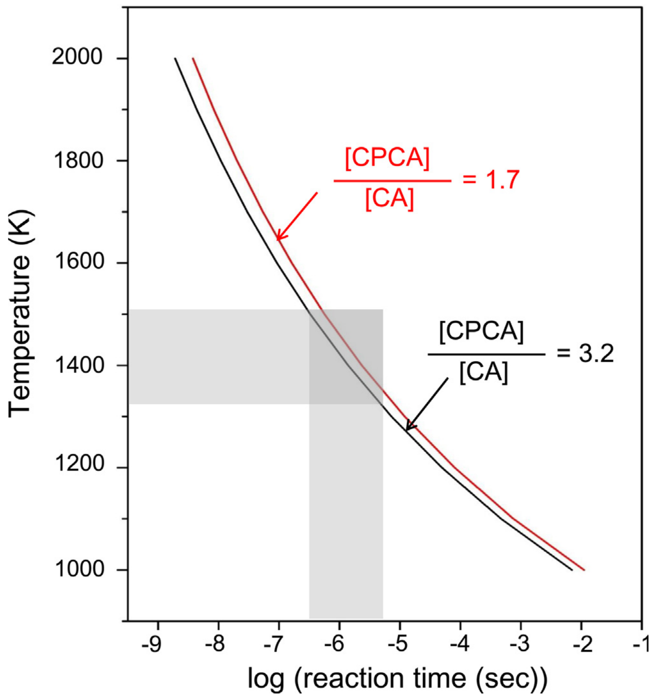

Fig. 7. The ratio of [CPCA] to [CP] generated from 2,3-DHF as a function of reaction temperature (K) and log (reaction time (s)). Black and red line represents the value of 3.2 and 1.7 for the [CPCA]/[CA] ratio, respectively. The theoretical rate constants for the relevant isomerization reactions are employed from Ref. [8].

6. The ratio of two competing product channels

As mentioned in Section 3.1, the ratio of CPCA production over CA production seems to be dependent on the excitation wavenumber: CPCA is more preferably produced, though the ratio of ~3.2 for C=C stretching region around 1590 cm^{-1} differs from that of ~1.7 for ring stretching and CC-H bending region around 1040 cm^{-1}. Because of the fluctuation of the output fluence effected by the daily conditions of FEL hardware, it would be unreasonable to discuss whether the difference of the product ratio is originated from the vibrational mode specificity of the parent molecule. The time profile of the parent and daughter molecules in Fig. 4b was measured at the laser fluence of ~5 mJ/macropulse, which was ~40% lower than the regular power used in Fig. 4a. The laser fluence could give an influence to the competition between two exit channels in IRMPA as reported by Ishikawa and Arai [20,21], who studied the effect of CO_2 laser fluence on the competing HF and HCl elimination channels in IRMPD of 1,2-dichloro-1,1-difluoroethane. In the lower fluence region, the HCl elimination process with a lower threshold energy is dominant. As the fluence increases, however, the HCl elimination process approaches saturation and the HF elimination process becomes more eminent.

Dubnikova and Lifshitz [8] calculated the rate constants for the following three unimolecular reactions with density functional theory;

$$\text{2,3-DHF to CPCA;}\quad k_1 = 6.31 \times 10^{14}\ \exp(-56.30 \times 10^3/RT)\ \text{s}^{-1}$$

$$\text{2,3-DHF to CA;}\quad k_2 = 4.57 \times 10^{14}\ \exp(-63.57 \times 10^3/RT)\ \text{s}^{-1}$$

$$\text{CPCA to CA;}\quad k_3 = 4.07 \times 10^{14}\ \exp(-58.88 \times 10^3/RT)\ \text{s}^{-1}$$

These theoretical rate constants reproduced reasonably the temperature dependence of the product ratio in the single pulse shock tube experiment [8]. Using the above rate constants and neglecting the reverse reactions, we evaluated the ratio [CPCA]/[CA] as a function of the reaction time and the temperature as depicted in Fig. 7. IR multiphoton dissociation dynamics of 2,5-DHF with CO_2 laser was studied by Chowdhury and Mittal [10]. They derived the value of $1.8 \times 10^6\ \text{s}^{-1}$ for the multiphoton decomposition of 2,5-DHF from the analysis of a transient UV absorption of the furan product, indicating that the lifetime of the hot 2,5-DHF is approximately on the μs order. Assuming a similar time scale for the isomerization of 2,3-DHF, the temperature giving the ratio [CPCA]/[CA] in the present experiment ranges from approximately from 1300 to 1500 K. This temperature range is higher than 900–1300 K for the shock wave experiment, and is lower than the vibrational temperature (~1800 K) of the nascent furan product from 2,5-DHF produced by CO_2 laser.

7. Summary

We studied infrared multiphoton dissociation and isomerization reactions of 2,3-dihydrofuran (2,3-DHF) in the gas phase with free electron laser at Tokyo University of Science (FEL-TUS). c-C_3H_5CHO (CPCA) and $CH_3CH{=}CHCHO$ (CA) were the main isomerization products. Action spectra for these products were red shifted by several tenth of cm^{-1} compared with FT-IR spectra of 2,3-DHF. From the measured [CPCA]/[CA] ratio, the temperature for the vibrationally hot 2,3-DHF was estimated to be 1300–1500 K.

The irradiation of FEL-TUS to CPCA as well as CA was also investigated. No isomerization reaction from *trans*-CA to CPCA and 2,3-DHF was recognized and the dissociation to propylene was the dominant process. From CPCA, both 2,3-DHF and CA were detected as isomerization products.

Quantum chemical calculations were carried out to evaluate the singlet potential energy surface for the unimolecular isomerization reactions of 2,3-DHF to propylene and CO. The production of CPCA and CA from 2,3-DHF was the unimolecular process through a single transition state, respectively. CA generated from 2,3-DHF was suggested to be a *cis*-conformer. The lack of transition states connecting *trans*-CA with 2,3-DHF or CPCA was consistent with the experimental results that the dissociation to propylene was the dominant route for CA. The conversion from CPCA to CA may proceed through a stepwise mechanism via energized 2,3-DHF or 3BA intermediate.

Acknowledgement

All the quantum chemical calculations were performed on computers owned by professor Y. Endo at the University of Tokyo.

Appendix A. Supplementary data

Supplementary data associated with this article can be found, in the online version, at http://dx.doi.org/10.1016/j.jphotochem.2016.02.014.

References

[1] A. Lifshitz, H. B-Hamou, Thermal reactions of cyclic ethers at high temperatures. 1. Pyrolysis of ethylene oxide behind reflected shocks, J. Phys. Chem. 87 (1983) 1782–1787.

[2] A. Lifshitz, M. Bidani, S. Bidani, Thermal reactions of cyclic ethers at high temperatures. 2. Pyrolysis of tetrahydrofuran behind reflected shocks, J. Phys. Chem. 90 (1986) 3422–3429.

[3] A. Lifshitz, M. Bidani, S. Bidani, Thermal reactions of cyclic ethers at high temperatures. 3. Pyrolysis of furan behind reflected shocks, J. Phys. Chem. 90 (1986) 5373–5377.

[4] A. Lifshitz, M. Bidani, S. Bidani, Thermal reactions of cyclic ethers at high temperatures. 4. Pyrolysis of 2,5-dihydrofuran behind reflected shocks, J. Phys. Chem. 90 (1986) 6011–6014.

[5] A. Lifshitz, M. Bidani, Thermal reactions of cyclic ethers at high temperatures. 5. Pyrolysis of 2,3-dihydrofuran behind reflected shocks, J. Phys. Chem. 93 (1989) 1139–1144.

[6] A. Lifshitz, A. Laskin, Isomerization of 2-methyl-4,5-dihydrofuran. Studies with a single-pulse shock tube, J. Phys. Chem. 98 (1994) 2341–2345.

[7] A. Lifshitz, C. Tamburu, Isomerization and decomposition of propylene oxide. Studies with a single-pulse shock tube, J. Phys. Chem. 98 (1994) 1161–1170.

[8] F. Dubnikova, A. Lifshitz, Isomerization of 2,3-dihydrofuran and 5-methyl-2,3-dihydrofuran: quantum chemical and kinetics calculations, J. Phys. Chem. A 106 (2002) 1026–1034.

[9] C. Karunatilaka, A.J. Shirar, G.L. Storck, K.M. Hotopp, E.B. Biddle, R. Crawley Jr., B.C. Dian, Dissociation pathways of 2,3-dihydrofuran measured by chirped-pulse Fourier transform microwave spectroscopy, J. Phys. Chem. Lett. 1 (2010) 1547–1551.

[10] P.K. Chowdhury, J.P. Mittal, IR multiphoton dissociation dynamics of 2,5-dihydrofuran. Time-resolved observation of concerted furan formation, Chem. Phys. Lett. 242 (1995) 421–426.

[11] Y. Miyamoto, T. Majima, S. Arai, H. Akagi, A. Maeda, H. Hata, K. Kuramochi, Y. Kato, K. Tsukiyama, ^{13}C-selective infrared multiple photon dissociation of β-propiolactone by a free electron laser, Nucl. Instr. Meth. Phys. Res. B 269 (2011) 180–184.

[12] T. Kanda, Y. Kato, T. Imai, K. Tsukiyama, Unimolecular isomerization from $(CH_3)_3C{-}N{=}C$ to $(CH_3)_3C{-}C{\equiv}N$ induced by infrared free electron laser, Nucl. Instr. Meth. Phys. Res. B 269 (2011) 1944–1946.

[13] S. Kuribayashi, A. Zako, Y. Matsumoto, S. Yamamoto, S. Arai, ^{13}C-selective infrared multiple photon decomposition of beta-propiolactone by use of a free electron laser, J. Nucl. Sci. Technol. 37 (2000) 959–962.

[14] J.L. Lyman, B.E. Newnam, T. Noda, H. Suzuki, Enrichment of silicon isotopes with infrared free-electron laser radiation, J. Phys. Chem. A 103 (1999) 4227–4232.

[15] J.K. Gibson, H.-S. Hu, M.J. van Stipdonk, G. Berden, J. Oomens, J. Li, Infrared multiphoton dissociation spectroscopy of a gas–phase complex of uranyl and 3-oxa-glutaramide: an extreme red-shift of the $[O{=}U{=}O]^{2+}$ asymmetric stretch, J. Phys. Chem. A 119 (2015) 3366–3374.

[16] M.J. van Stipdonk, K. Patterson, J.K. Gibson, G. Berden, J. Oomens, IRMPD spectroscopy reveals a novel rearrangement reaction for modified peptides that involves elimination of the N-terminal amino acid, Int. J. Mass Spect. 379 (2015) 165–178.

[17] M.U. Ehsan, Y. Bozai, W.L. Pearson III, N.A. Horenstein, J.R. Eyler, Infrared multiple photon dissociation spectrum of protonated bis(2-methoxyethyl) ether obtained with a tunable CO_2 laser, Phys. Chem. Chem. Phys. 17 (2015) 25877–25881.

[18] A. Hartford Jr., S.A. Tuccio, Nitrogen isotope enrichment via infrared laser induced isomerization of methyl and ethyl isocyanide, Chem. Phys. Lett. 60 (1979) 431–434.

[19] MOLPRO is a package of ab initio programs written by H.-J. Werner, P. J. Knowles, G., Knizia, F. R. Manby, M. Schütz, P., Celani, T., Korona, R., Lindh, A., Mitrushenkov, G., Rauhut, K. R. Shamasundar, T. B. Adler, R. D. Amos, A., Bernhardsson, A., Berning, D. L. Cooper, M. J. O. Deegan, A. J. Dobbyn, F., Eckert, E., Goll, C., Hampel, A., Hesselmann, G., Hetzer, T., Hrenar, G., Jansen, C. Köppl, Y., Liu, A. W. Lloyd, R. A. Mata, A. J. May, S. J. McNicholas, W., Meyer, M. E. Mura, A. Nicklaß, D. P. O'Neill, P., Palmieri, D., Peng, K. Pflüger, R., Pitzer, M., Reiher, T., Shiozaki, H., Stoll, A. J. Stone, R., Tarroni, T., Thorsteinsson, M. Wang.

[20] Y. Ishikawa, S. Arai, Competition between HF And HCl molecular elimination in IRMPD of 1,2-dichloro-1,2-difluoroethane, Chem. Phys. Lett. 103 (1983) 68–72.

[21] Y. Ishikawa, S. Arai, Competition between hydrogen fluoride and hydrogen chloride molecular elimination channels in the infrared multiple-photon decomposition of 1,2-dichloro-1,1-difluoroethane, Bull. Chem. Soc. Jpn. 57 (1984) 681–686.